Journal of Geography and Cartography (2023) Volume 6 Issue 2
doi: 10.24294/jgc.v6i2.2358

ORIGINAL RESEARCH ARTICLE

GNSS-Interferometric Reflectometry, spectral artifacts and sea level measurements in the Mediterranean Sea

Roberto Devoti*, Sergio Bruni, Grazia Pietrantonio

Istituto Nazionale di Geofisica e Vulcanologia, Osservatorio Nazionale Terremoti, 00143 Rome, Italy

*** Corresponding author:** Roberto Devoti, roberto.devoti@ingv.it

ABSTRACT

Tidal sea level variations in the Mediterranean basin, although altered and amplified by resonance phenomena in confined sub-basins (e.g., Adriatic Sea), are generally confined within 0.5 meters and exceptionally up to 1.5 meters. Here we explore the possibility of retrieving sea level measurements using data from GNSS antennas on duty for ground motion monitoring and analyze the spectral outcomes of such distinctive measurements. We estimate one year of GNSS data collected on the Mediterranean coasts in order to get reliable sea level data from all publicly available data and compare it with collocated tide gauges. A total of eleven stations were suitable for interferometric analysis (as of 2021), and all were able to supply centimeter-level sea level estimates. The spectra in the tidal frequency windows are remarkably similar to tide gauge data. We find that the O_1 and M_2 diurnal and semidiurnal tides and MK_3, MS_4 shallow sea water tides may be disturbed by aliasing effects.

keywords: GNSS Reflectometry; sea level variations; tides; Mediterranean Sea

ARTICLE INFO

Received: 3 July 2023
Accepted: 4 August 2023
Available online: 28 September 2023

1. Introduction

Sea level is considered an Essential Ocean Variable (EOV) by the Global Ocean Observing System[1]. Since the 19th century, tide gauges have been a key procedure to monitor the sea level. Tide gauges measure the relative sea level (RSL) with respect to a local reference on land and are currently used to study mean sea level variations, assess anomalous events, make tidal predictions, develop geodetic applications, and support harbor operations and navigation. RSL is a combination of global sea level variations and local vertical land motion; tide gauges only measure the sea level with respect to the local ground, without regard to ground movement. As demonstrated by Larson et al.[2], sea surface height can be monitored at the level of a few centimeters using a single GNSS antenna facing the seashore. In that case, the local reference point matches the GNSS antenna mount, which can be monitored directly in a global reference frame. Therefore, the GNSS-derived sea level is consistently an absolute measurement, sensitive to the absolute sea level trend. The technique is based on the Interferometric Reflectometry (IR) process and uses the signal-to-noise ratio (SNR) measured for each GNSS carrier frequency. The SNR, recorded for each GNSS satellite's carrier frequency, contains a characteristic interference pattern caused by the signal reflection on a planar reflector underlying the GNSS antenna, i.e., the sea surface, and is proportional to the reflector's height. Thus, sea level variations become available through the analysis of GNSS-SNR data. We

screened all existing GNSS stations in the Mediterranean area to assess the feasibility and precision of the technique. For those stations that allow the estimation of sea level, we estimate one year of sea level variations (2021) and compare it to the nearest tide gauge.

2. Data source and analysis methods

In the Mediterranean area, EUREF (European Geodetic Reference Frame) and other national-based GNSS networks usually provide high-quality observations aimed at obtaining time series of precise positions. We select all sites located very close to the seashore in which the antenna height does not exceed 20 m from the sea surface. We limit the observations to very low elevation angles (<30°) and adopt a proper azimuthal mask for each site in order to maximize sea surface visibility, avoiding obstructions or other sources of reflection on the ground. All GNSS data analyzed in this work is available on the web (verified on 31 December 2022).

We estimate sea-level variations using the "gnssrefl" open source software available on the github platform (https://github.com/kristinemlarson/gnssrefl[3]). The software extracts the SNR data from the RINEX raw data and analyzes the interference pattern caused by the beating signal between the direct and reflected GNSS signal during satellites' rising and setting periods. It performs the analysis for each available carrier frequency and for each available satellite in any given range of elevation and azimuthal angles. The azimuth-elevation mask is easily restricted using the web app developed by the GNSS-IR research group (https://gnss-reflections.org/rzones). It allows for visualizing actual reflection zones in the surroundings of the GNSS antenna and determining the optimal azimuth and elevation ranges. The analysis software then estimates the reflector height (i.e., the sea level height) at each satellite pass and for each carrier frequency, crossing the azimuth-elevation sector. This produces a time series of reflector heights (RH) determined at times of the satellite's pass that represents the raw GNSS estimates of the sea level. Since the sea surface is not stationary during the satellite's pass, all height determinations are corrected for the instantaneous sea-level variation (Hdot correction, Larson et al.[4]). We adopt a running box average to smooth the sea level time series, using a sliding window of 2–3 h, depending on the noise content of the series.

The number of daily sea level determinations depends mainly on the sea surface visibility and the number of satellites tracked by the receiver; we generally observe an average of 60 to 200 determinations per day (see **Table 1**). High sampling rates allow sub-daily tidal determinations, but, at the same time, the estimates are unevenly sampled since the satellite's transits do not repeat at regular time intervals.

Table 1. GNSS stations analyzed in this study, among all public stations only 11 allow reliable sea level variations estimation. The last two columns in the table report the correlation coefficient computed among sea level estimates and Tide Gauges data, and the relative noise. i.e., the standard deviation of differences.

Place	Site ID	Net	Sats	Lat (°)	Lon (°)	N.obs day[1)]	Average height	Tide gauge	Corr (%)[2)]	Noise (cm)
Barcelona, ES	BCL1	IGNE	G, R, E, C	41.3418	2.1657	112	7.0	Barcelona, ES	96.2	2.9
Melilla, ES	MLLL	IGNE	G,R,E,C	35.2907	−2.9285	218	4.9	Melilla, ES	94.8	2.9
Tarifa, ES	TAR0	EUREF	G,R,E	36.0086	−5.6027	132	8.6	Tarifa, ES	98.4	4.8
S.Severa, FR	LURI	RGP	G,R	42.8884	9.4759	66	6.0	Centuri, FR	90.5	5.1
Tarragona, ES	TRRG	IGNE	G,R,E,C	41.0790	1.2132	55	6.0	Tarragona, ES	85.0	5.7
Alicante, ES	ALAC	EUREF	G,R,E,C	38.3389	−0.4812	126	13.5	Alicante, ES	83.2	7.4
Sète, FR	SETE	RENAG	G,R,E	43.3976	3.6991	68	5.5	Sète, FR	84.0	8.0
Mallorca, ES	MAL1	IGNE	G,R,E,C	39.5602	2.6375	63	5.0	Mallorca, ES	79.6	8.3
P.Garibaldi, IT	GARI	EUREF	G,R,E,C	44.6769	12.2494	67	7.7	Ravenna, IT	87.9	8.3
Poreč, HR	PORE	EUREF	G,R,E	45.2260	13.5951	58	22.1	Venezia19, IT	90.9	10.5
Venezia, IT	VEN1	EUREF	G,R,E,C	45.4306	12.3541	128	16.9	Venezia19, IT	92.0	11.3

1) N.obs day: Average number of observations per day;
2) Corr: correlation

Among all the public GNSS permanent stations, we found only eleven stations suitable for the GNSS-IR analysis (see **Figure 1**). The most common factors that prevent sea level determinations are: 1) the absence of SNR observations registered in the RINEX files; 2) a high elevation mask, typically set to 10°; and finally, 3) an unfavorable position or reduced sea surface visibility. Most of the receivers considered in this work have multi-constellation tracking capability (at least GPS, Glonass, and Galileo), and almost all of them are located within a short distance (less than 20 km) from an active tide-gauge station. The sea level estimates are compared and cross-correlated with the nearest tide gauge data. The cross-correlation procedure foresees the following steps: both the GNSS and Tide-gauge time series are smoothed through a moving average filter using a 3-hour sliding window in order to filter out the high-frequency signal. The filtered series were then linearly interpolated at hourly time intervals, and eventual data gaps were discarded in both time series. Finally, we used the Matlab® function *xcorr* to compute the normalized cross-correlation among the two series. Note that the correlation coefficient encompasses the daily tidal signatures since the smoothing procedure does not alter the diurnal and sub-diurnal tidal bands. The same interpolated series are then used to compute residuals and assess the relative agreement of the sea-level measurements. The GNSS-IR and Tide-Gauge time series are aligned by subtracting an arbitrary average value computed over the entire observation period.

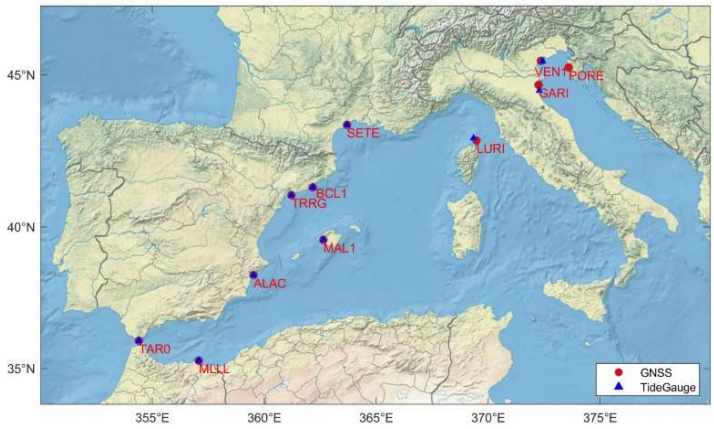

Figure 1. Map of the Mediterranean region showing the GNSS stations (red circles) and tide gauges (blue triangles) considered in this work.

We also compare the spectra of the GNSS and tide gauge data in order to evaluate the sensitivity of the GNSS-IR data at different frequencies. We evaluate the Lomb-Scargle periodogram using the "plomb" function of Matlab® software[5]. This algorithm is able to deal with unevenly and randomly sampled data. The first requirement is undoubtedly met for GNSS reflection observations since they rely on the satellite's pass and cannot be regularly sampled; instead, random sampling is generally not met because satellites do exhibit systematic revisit periods. Hence, the sea level data are somehow in between evenly and randomly sampled data. A simple test conducted on a synthetic signal will clarify some theoretical aspects of non-randomly sampled data in Appendix A. In paragraph 4, we briefly discuss the effects of GNSS constellation periodicities on the sea level periodograms.

3. Sea level results

In **Figure 2**, we show the sea-level time series obtained at Melilla, the autonomous city of Spain in North Africa (GNSS station MLLL is located on the edge of a large pier in the port of Melilla). The color of sea-level markers shows the satellite's constellations that contribute to the estimation; in this case, all four constellations are useful for IR observations throughout the year. In the bottom panel of **Figure 2**, the GNSS time series is compared with mareographic data recorded from a station located a few meters away from the GNSS antenna. In this case, we observe an average discrepancy of about 3 cm between the GNSS and tide gauge data. The sea level variations of all stations are reported in supplementary **Figure 1S**, where the

observations are distinguished by satellite constellations. In general, at least three constellations (GPS, GALILEO and GLONASS) are always available, and for half of the stations, BEIDOU satellites are also available. The number of observed satellites depends on the tracked frequencies of the GNSS receiver; each constellation contributes a few tens of observations per day (see supplementary **Figure 2S**), the most prolific being the GPS satellites. On average, most of the stations provide 2–3 observations per hour, all over the day (see supplementary **Figure 3S**).

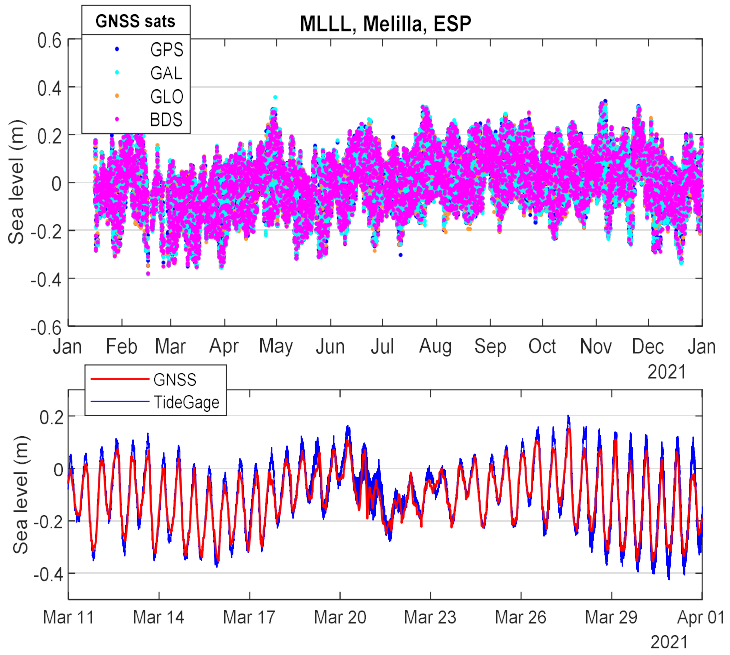

Figure 2. Top, one year of GNSS-IR Sea level estimates (different colors for each satellite constellation) at Melilla GNSS station (MLLL, IGNE network). Bottom, a zoom at mid of March for the same data compared with sea level data observed at the collocated tide gauge (Meli).

Not all stations yield similar residuals; the noise of the sea-level measurements depends partly on the nearby freight activities. Harbors and piers, where GNSS antennas are usually hosted, may be very busy environments in which marine traffic, boat docking, and cargo operations cause odd reflections that may bias the measurements in different ways. **Table 1** summarizes the results in terms of residuals for all stations analyzed in this study. We define the discrepancy as the standard deviation (STD) of residuals between the GNSS and tide gauge sea levels, both series interpolated at hourly values. The best agreement has been observed for BCL1 and MLLL stations (Barcelona and Mellilla, respectively), both showing 29 mm of STD. The worst agreement is found at VEN1 (Venezia, Italy) with 113 mm, but here the tide gauge is located just outside the lagoon of Venice, whereas the GNSS antenna is facing the "Canal Grande" inside the lagoon at a distance of a distance of 5 km from the tide gauge. Thus, we expect these differences to be caused principally by different tidal responses at these two sites. The overall correlation coefficient computed over the entire year of data is always greater than 80%, approaching 98% in the best case (see **Table 1**).

In **Figure 3**, we display the spectral coherence obtained after stacking all GNSS results in order to get a global overview at different frequencies. The most outstanding coherence is in the diurnal and semidiurnal bands (>75%), i.e., where the strongest gravitational tidal constituents are effective. Lower coherence (10%–20%) is observed in the ter-diurnal and quarter-diurnal bands, where GNSS shows a certain degree of coherence with these particular overtides and compound tides caused by shallow water effects. As an example, we illustrate in **Figure 4** the spectrum of station TAR0 (Tarifa, Spain); all others are reported in supplementary **Figure 5S**. The spectra are limited to four main spectral windows (near 1-2-3-4 cycles/day), and both the GNSS and tide gauge sea level spectra are overlayed on the same graph. In the diurnal band, the K_1 tide (luni-

solar diurnal) is dominant, and P_1 (solar diurnal) and O_1 (lunar diurnal) are in most cases recognizable, although below the 1% threshold. The major tidal constituent is usually in the semidiurnal band M_2 (lunar semidiurnal), related to the direct gravitational effect of the moon, which results in two highs every 24 h and 50 min. Minor constituents are S_2 (solar semidiurnal) and N_2 (lunar semidiurnal), which are visible well above the detection threshold for all stations. Higher frequencies are due to tidal distortion caused by shallow water effects, making the tides asymmetric so that tidal rise and fall are no longer equal. The ter-diurnal constituents, although recognizable by tide gauge and GNSS data, are always below the threshold and barely visible. Quarter diurnal constituents are almost ubiquitous, in which the M4 overtide and the compound tides MN4 and MS4 are significant in a few stations.

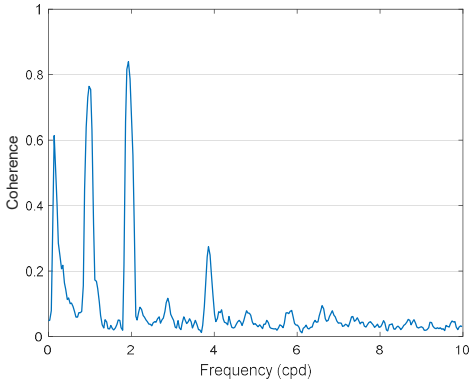

Figure 3. Stacked spectral coherence of the GNSS sea level data for all 11 stations considered. Coherence is normalized, frequency is expressed in units of cycles per day.

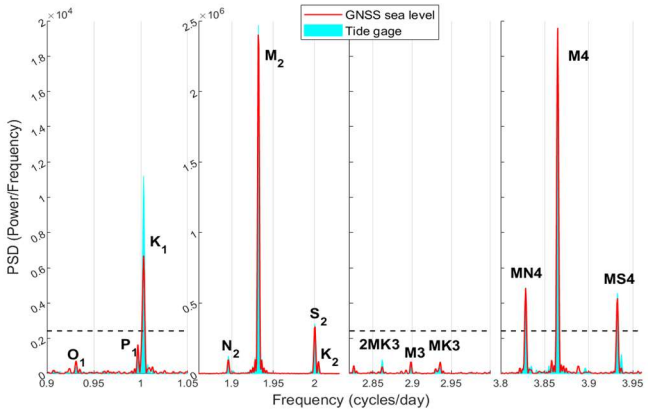

Figure 4. Spectra of one year of sea level determinations at TAR0 (Tarifa, ESP) GNSS station and tide gauge data. Tidal frequencies of the diurnal, semidiurnal, ter-diurnal and quarter diurnal constituents are shown respectively from left to right panels. Red line refers to the GNSS data and cyan line to the tide gauge data. The horizontal dashed line represents the 1% confidence level of the spectral amplitudes.

4. Spectral leakage of GNSS-IR sea level data

Here we will briefly summarize a spectral feature that is very peculiar for GNSS data and may represent a source of confusion and misunderstanding of the results. GNSS satellites operate in almost circular orbits at altitudes of about 20,000 km and orbital periods of almost half of a sidereal day (i.e., the sidereal day is the time the Earth takes to complete one rotation about its axis with respect to fixed stars). Because of the prograde orbits, the GNSS satellites' revisit time (i.e., the time satellites need to pass over again, as viewed from the Earth) is close to one sidereal day. Moreover, GALILEO, GLONASS, and BEIDOU satellites are arranged into three different orbital planes, each nominally eight satellites having orbital periods of respectively 14 h 05', 11 h 16', and 12 h 53'. Whereas GPS satellites are distributed over six orbital planes, each containing each four satellites, with a revolution period of nearly 11 h 58', very close to half a sidereal day (11 h 58' 02").

To get a rough idea of possible revisit times for satellites belonging to a given constellation, we can form integer combinations of the two fundamental oscillations, the satellite orbital period and the Earth rotation period. This dependency may formally be explicited as:

$$f_r = |nf_S + mf_E| \text{ and } n, m = \cdots, -2, -1, 0, 1, 2, \ldots \quad (1)$$

where f_E is the Earth rotation frequency and f_S is the orbital frequency and f_r are the resonance frequencies. Equation (1) identifies a family of GNSS system-specific signals that could affect the sampling rate of the observations. Such spurious signals, not correlated with sea level variations, are clearly visible in our spectra at different frequencies. As an example, the spectra for station BCL1 (Barcelona, Spain) are shown in **Figure 5** for different satellite constellations. The satellite-specific resonant frequencies (Equation 1)) are indicated as grey vertical bars. The lowest frequency represents the fundamental revisiting frequency for that specific constellation, a sort of "beating frequency" that combines an integer number of Earth rotations and orbital revolutions. In terms of period, the revisiting frequency represents the smallest number of sidereal days that contain an integer number of orbits. All higher system-specific frequencies are harmonics (overtones) of this fundamental frequency. Assuming the aforementioned orbital periods for the respective GPS, GLONASS, GALILEO, and BEIDOU constellations, we recognize the following revisiting frequencies: 2 orbits per day, 17 orbits every 8 days, 17 orbits every 10 days, and 13 orbits every 7 days. Resonances and aliasing produced by such signals on different geodetic parameters are well documented in the literature[6–11]. In particular, Ray et al.[11] first proposed a mechanism that involves the repeating geometry of the satellite constellation with respect to the tracking stations. The authors observe that the daily advance of the orbital repeat geometry causes an alias period of 350 days for the GPS constellation, so that any observational bias (such as multipath) could be expected to repeat at such an aliasing period. Of course, since the sea level parameters are derived from the interaction of multipath disturbances on the recorded GNSS signal, we expect that these observations are strongly affected by the satellite's repeating frequencies.

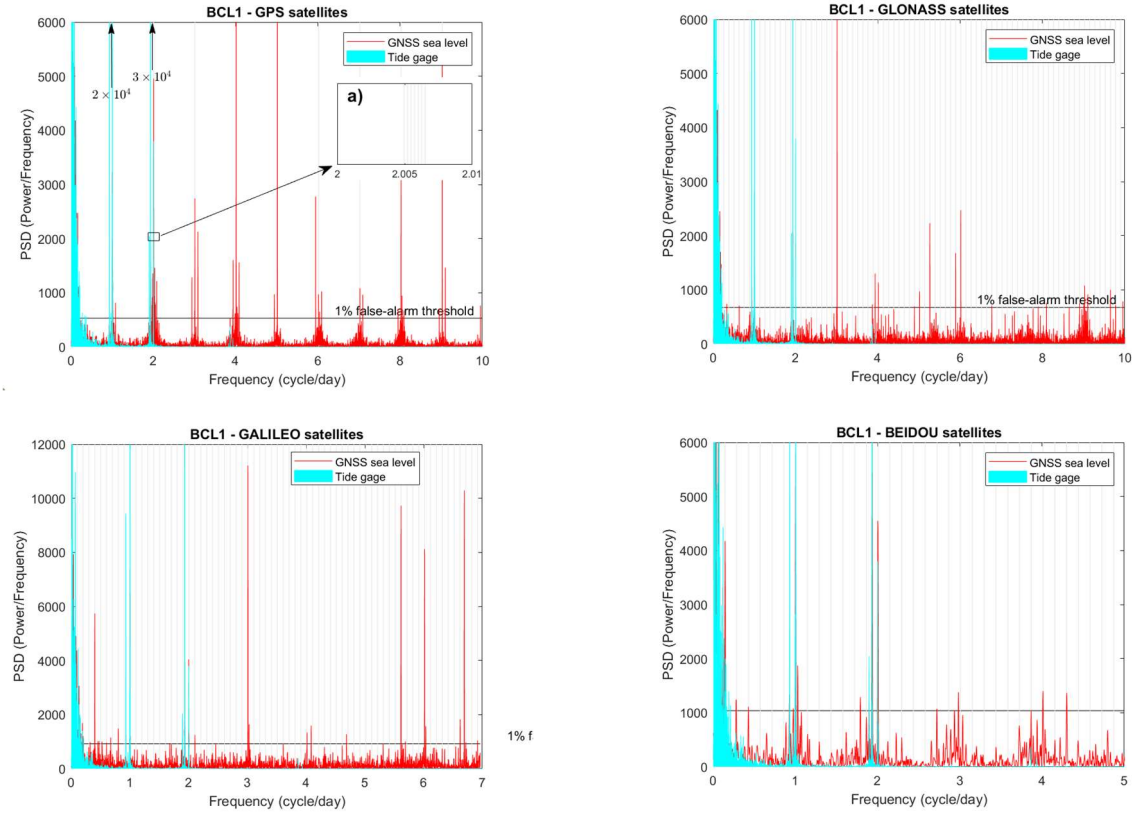

Figure 5. Spectrum of BCL1 sea level data (red) and tide gauge data (cyan) at Barcelona harbor obtained with different constellation data (GPS, GLONASS, GALILEO and BEIDOU). Grey vertical lines indicate the family of system resonances for the given constellation, the inlet a), zooming at 2 cpd, shows the fine structure of the resonance for the GPS constellation).

This kind of leakage in the spectra can be reduced by interpolating the estimated time series at regular time intervals. In **Figure 6,** we show the spectra relevant to four different stations obtained from GPS observations only. The raw sea level data provide the dotted line, whereas the interpolated data provide the solid line spectra. The effect of sampling leakage disappears below the significance level when the signal is re-sampled at evenly spaced time stamps, demonstrating the fictitious nature of such overtones. The critical issue is that the leakage frequencies appear to be very close to the major tidal frequencies K_1, P_1, K_2, and S_2 (at 1 and 2 cpd) and partly overlap with them. For this reason, the amplitude and frequencies of tidal components have to be interpreted with caution in GNSS-IR estimates.

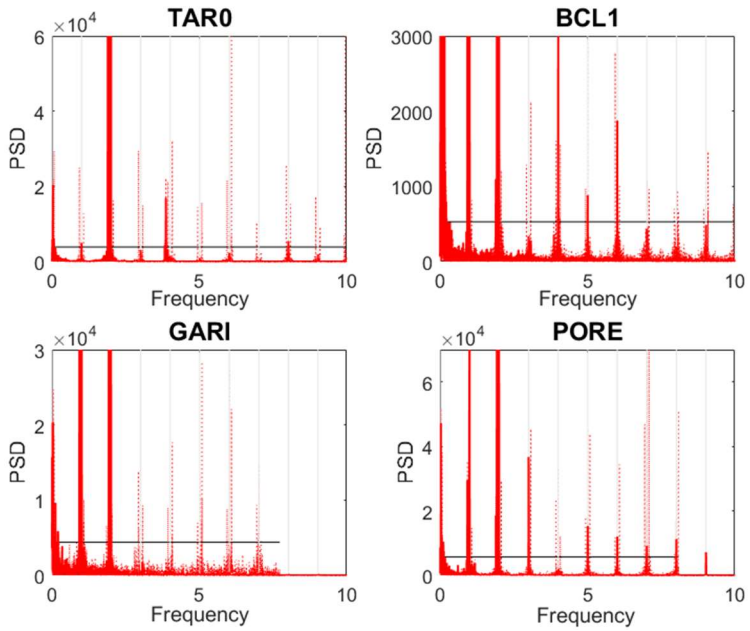

Figure 6. Spectra of Sea level data obtained from GPS data at four different stations.

5. Discussion and conclusions

The GNSS-IR sea level estimation in the Mediterranean area is feasible at the level of a few centimeters of precision (ranging from 30 mm up to a hundred millimeters), consistent with similar findings in the literature[2,12–14]. The repeatabilities of sea level estimates, referenced with respect to tide gauge data, are summarized in **Table 1** for the eleven GNSS stations considered in this study. The best-performing stations are characterized by good visibility of the sea surface, a relatively quiet environment with limited vessel traffic, and being equipped with multi-satellite observing capabilities. All eleven GNSS stations sample multi-constellation observations at 30 s and are effective for sea-level recovery all around the year. The antenna heights range from a few meters above sea level to 22 m at the PORE station. Most of the stations belong to the EUREF permanent network and the IGNE network in Spain. The majority of permanent stations located on the Mediterranean coasts lack at least one of the aforementioned conditions and cannot provide reliable sea level estimates. Diurnal and semidiurnal frequencies are the most outstanding tidal signals with the dominant K_1 and M_2 tides, but non-linear tidal components resulting from the interaction of major tides with the shallow sea are clearly visible in the spectra. The ter-diurnal constituents are generally below the detection threshold, and the quarter-diurnal tides, i.e., the M_4 overtide and the MN_4 and MS_4 compound tides, are recognizable in a few stations.

We note that sampling satellite's observables from the rotating Earth induce strong aliasing effects in the spectral output of sea-level estimates; in particular, the GPS-derived estimates show severe aliasing effects causing spectral overtones at multiples of the sidereal frequency (see **Figures 5** and **6**). The aliased spikes

occur close to the diurnal O_1 and semidiurnal M_2 astronomical tides and near the non-linear MK_3 and MS_4 tidal components. Thus, it suggests a careful interpretation of those spectral components whenever the sea levels are determined by means of GPS observations.

Space geodesy is the only tool that may establish a global reference frame in which to express local sea level data in a long-term, consistent, and global reference frame. For this reason, GNSS stations located on coasts are useful for climate change and coastal hazard studies. The present analysis recognizes only a limited number of GNSS stations available in the Mediterranean area for GNSS-IR studies. The feasibility of interferometric reflection depends critically on the location of the GNSS antenna in proximity to the coast, the visibility of the sea surface, and the environmental noise.

Supplementary materials

As supplementary material we plot a series of station parameters to characterize the sea-level determinations at each of the 11 sites considered in this work (i.e., the number of observations per day and for different satellite constellations; the number of observations per hour stacked in the 24-hour window; the sea-level spectral lines in the diurnal semi, ter, quater-diurnal frequency windows).

In addition, we furnish the sea-level time series for all 11 stations as column-formatted ASCII files.

Author contributions

Conceptualization, RD, data curation and data analysis, RD, SB and GP; writing—original draft preparation, RD, writing—review and editing, GP. All authors have read and agreed to the published version of the manuscript.

Acknowledgments

This work was partially supported by Clypea program—Innovation Network for Future Energy, of the Italian Ministry of Ecological Transition and the GAIA project—Geomorphological and hydrogeological vulnerability of Italian coastal areas in response to sea level rise and marine extreme events (PRIN 2023, Progetti di Ricerca di Interesse Nazionale).

Conflict of interest

The authors declare no conflict of interest.

Data availability

The original GNSS raw data are available on the following public web sites (see **Table 1** to cross-reference the network):

EUREF: https://www.epncb.oma.be/

IGNE: ftp://ftp.geodesia.ign.es/ERGNSS

RGP: ftp://rgpdata.ign.fr/pub/data

RENAG: ftp://renag.unice.fr/data

We download the Tide-gauge data from the Intergovernmental Oceanographic Commission web site:

IOC: http://www.ioc-sealevelmonitoring.org

The sea level datasets estimated from GNSS data in the current study are available in the supplementary material as simple ASCII files.

References

1. EuroGOOS. Sea level observation networks in and around Europe. Available online: https://eurogoos.eu/download/eurogoos-tide-gauge-note-to-policy-2017 (accessed on 1 July 2023).
2. Larson KM, Löfgren JS, Haas R. Coastal sea level measurements using a single geodetic GPS receiver. *Advances in Space Research* 2013; 51(8): 1301–1310. doi: 10.1016/j.asr.2012.04.017
3. Roesler C, Larson KM. Software tools for GNSS Interferometric Reflectometry. *GPS Solutions* 2018; 22: 80. doi: 10.1007/s10291-018-0744-8
4. Larson KM, Ray RD, Nievinski FG, Freymueller JT. The accidental tide gauge: A GPS reflection case study from Kachemak Bay, Alaska. *IEEE Geoscience and Remote Sensing Letters* 2013; 10(5): 1200–1205. doi: 10.1109/LGRS.2012.2236075
5. Press WH, Rybicki GB. Fast algorithm for spectral analysis of unevenly sampled data. *Astrophysical Journal* 1989; 338(1): 277–280. doi: 10.1086/167197
6. Zajdel R, Sośnica K, Bury G, et al. System-specific systematic errors in earth rotation parameters derived from GPS, GLONASS, and Galileo. *GPS Solutions* 2020; 24: 74. doi: 10.1007/s10291-020-00989-w.
7. Griffiths J, Ray JR. Sub-daily alias and draconitic errors in the IGS orbits. *GPS Solutions* 2013; 17(3): 413–422. doi: 10.1007/s10291-012-0289-1
8. Collilieux X, Métivier L, Altamimi Z, et al. Quality assessment of GPS reprocessed terrestrial reference frame. *GPS Solutions* 2011; 15(3): 219–231. doi: 10.1007/s10291-010-0184-6
9. Penna NT, Stewart MP. Aliased tidal signatures in continuous GPS height time series. *Geophysical Research Letters* 2003; 30(23): 2184. doi: 10.1029/2003GL018828
10. Dong D, Fang P, Bock Y, et al. Anatomy of apparent seasonal variations from GPS derived site position time series. *Journal of Geophysical Research* 2002; 107(B4): ETG 9-1–ETG 9-16. doi: 10.1029/2001JB000573
11. Ray JR, Altamimi Z, Collilieux X, van Dam T. Anomalous harmonics in the spectra of GPS position estimates. *GPS Solutions* 2008; 12(1): 55–64. doi: 10.1007/s10291-007-0067-7
12. Löfgren JS, Haas R, Scherneck HG. Sea level time series and ocean tide analysis from multipath signals at five GPS sites in different parts of the world. *Journal of Geodynamics* 2014; 80: 66–80. doi: 10.1016/j.jog.2014.02.012
13. Larson KM, Ray RD, Williams SDP. A 10-Year comparison of water levels measured with a geodetic GPS receiver versus a conventional tide gauge. *Journal of Atmospheric and Oceanic Technology* 2017; 34(2): 295–307. doi: 10.1175/JTECH-D-16-0101.1.
14. Dahl-Jensen TS, Andersen OB, Williams SDP, et al. GNSS-IR Measurements of inter annual sea level variations in Thule, Greenland from 2008–2019. *Remote Sensing* 2021; 13(24): 5077. doi: 10.3390/rs13245077